

## Article

# Comparison of 24 h Surface Ozone Forecast for Poland: CAMS Models vs Simple Statistical Models with Limited Number of Input Parameters

Izabela Pawlak <sup>1,\*</sup>, Alnilam Fernandes <sup>1</sup>, Janusz Jarosławski <sup>1</sup>, Krzysztof Klejnowski <sup>2</sup> and Aleksander Pietruczuk <sup>1</sup>

<sup>1</sup> Institute of Geophysics, Polish Academy of Sciences, 01-452 Warszawa, Poland

<sup>2</sup> Institute of Environmental Engineering, Polish Academy of Sciences, 41-819 Zabrze, Poland

\* Correspondence: izap@igf.edu.pl

**Abstract:** Surface ozone is usually measured in national networks, including the monitoring of gaseous components important for determining air quality and the short-term forecast of surface ozone. Here we consider the option of forecasting surface ozone based on measurements of only surface ozone and several weather parameters. This low-cost configuration can increase the number of locations that provide short-term surface ozone forecast important to local communities. 24 h prediction of the 1-h averaged concentration of surface ozone were presented for rural (Belsk, 20.79° E, 51.84° N) and suburban site (Racibórz, 18.19° E, 50.08° N) in Poland for the period 2018–2021 via simple statistical models dealing with a limited number of predictors. Multiple linear regression (MLR) and artificial neural network (ANN) models were examined separately for each season of the year using temperature, relative humidity, an hour of the day, and 1-day lagged surface ozone values. The performance of ANN (with  $R^2 = 0.81$  in Racibórz versus  $R^2 = 0.75$  at Belsk) was slightly better than the MLR model (with  $R^2 = 0.78$  in Racibórz versus  $R^2 = 0.71$  at Belsk). These statistical models were compared with advanced chemical–transport models provided by the Copernicus Atmosphere Monitoring Service. Despite the simplicity of the statistical models, they showed better performance in all seasons, with the exception of winter.

**Keywords:** surface ozone; forecast; statistical models; chemistry–transport models; air quality

**Citation:** Pawlak, I.; Fernandes, A.; Jarosławski, J.; Klejnowski, K.; Pietruczuk, A. Comparison of 24 h Surface Ozone Forecast for Poland: CAMS Models vs Simple Statistical Models with Limited Number of Input Parameters. *Atmosphere* **2023**, *14*, 670. <https://doi.org/10.3390/atmos14040670>

Academic Editor: Chang H. Jung

Received: 10 February 2023

Revised: 18 March 2023

Accepted: 26 March 2023

Published: 31 March 2023



**Copyright:** © 2023 by the authors. Licensee MDPI, Basel, Switzerland. This article is an open access article distributed under the terms and conditions of the Creative Commons Attribution (CC BY) license (<https://creativecommons.org/licenses/by/4.0/>).

## 1. Introduction

Surface ozone ( $O_3$ ) is a secondary photochemical pollutant at the ground level of the atmosphere [1]. The primary source of surface  $O_3$  is photochemical production, including nitrogen oxides ( $NO_x$ ), carbon monoxide (CO), and volatile organic compounds (VOC) [2–4]. The other sources are the downward transport of stratospheric ozone into the troposphere [5,6] and the long-range transport of surface  $O_3$  from distant polluted areas [7]. The dominant sink of surface  $O_3$  are processes of photochemical destruction and the mechanism of dry deposition on different surfaces [8]. Surface  $O_3$  shows non-linear dependence on the concentration of its precursors [9]. It could be classified into two chemical regimes,  $NO_x$  saturated, and  $NO_x$  limited, which are determined by the sensitivity of surface  $O_3$  to anthropogenic precursors [10]. Surface  $O_3$  can decrease as  $NO_x$  decreases under  $NO_x$  saturated regime or as  $NO_x$  increases under  $NO_x$  limited regime. The increase of VOC generally leads to an increase of surface  $O_3$  regardless of the kind of regime. The main sources of  $NO_x$  and VOC are traffic and biogenic emissions, respectively. Hence, the surface  $O_3$  concentrations can vary significantly between rural and urban locations. Many studies have shown higher surface  $O_3$  concentrations in rural areas compared to urban areas [11–13]. The chemistry of  $NO_x$ , VOC, and  $O_3$  in the troposphere and their relationship is well known and extensively discussed in the literature [9,14].

Surface O<sub>3</sub> plays an important role in the atmosphere. It is an important greenhouse gas with a radiative forcing of  $0.40 \pm 0.20$  W/m<sup>2</sup> [15] and a major component of photochemical smog [16]. High levels of surface O<sub>3</sub> have an adverse effect on human health and vegetation [17–19]. Ozone photolysis processes play an important role in the troposphere as a source of hydroxyl radicals (OH)—a dominant atmospheric oxidant [20].

Surface O<sub>3</sub> formation and transport are strongly influenced by meteorological conditions. Temperature affects the rate of chemical reactions, the lifetime of polyacrylonitrile (PAN) compounds (functioning as a reservoir of NO<sub>x</sub>) as well as affects the emission of VOC [21,22]. Solar radiation initiates photochemical processes [23]. An increase in relative humidity promotes the formation of clouds [24] and affects the stomatal conductivity of the leaves. In response to the increase in humidity, the stomata open, which increases the absorption of surface O<sub>3</sub> in the processes of dry deposition [25,26]. A detailed description of the connection between particular meteorological parameters has been broadly documented in the literature [1,27–29].

Surface O<sub>3</sub> can be predicted with the use of statistical and deterministic methods [30]. The ability of both methods to predict the surface O<sub>3</sub> variability as a result of changes in precursor emissions and ambient meteorological conditions is very important, especially nowadays, in a changing climate. Quantifying surface O<sub>3</sub> response to meteorological changes is a particular challenge [31]. The prediction of surface O<sub>3</sub> is further complicated by its nature as a secondary pollutant [32].

Chemistry–transport models (CTM) are commonly used to forecast surface O<sub>3</sub> variability [33,34]. However, their use is limited because they require huge computational resources and suffer from a large bias resulting from the coarse resolution [35], especially in urban areas with changing chemistry, varied topography, and uncertainty of emission inventory [36]. Therefore, statistical models, e.g., multiple linear regression (MLR) and artificial neural network (ANN), can be an additional tool supporting surface O<sub>3</sub> prediction.

A number of works have compared MLR and ANN methods for surface O<sub>3</sub> prediction starting from the early 1990s. Yi and Prybutok [37] developed ANN, linear regression model, and Box-Jenkins ARIMA to predict the surface O<sub>3</sub> maximum between 1993–1994 in Dallas. Comrie [38] investigated the potential of MLR and ANN to predict daily surface O<sub>3</sub> concentration between 1991 and 1995 for eight cities around the United States. Spellman [39] used MLR and ANN models to predict spring-summer surface O<sub>3</sub> (from May to September) in the period 1993–1996 for five different sites (remote, rural, and urban center) in the UK. Gardner and Dorling [40] used MLR, regression tree, and ANN models to predict hourly surface O<sub>3</sub> values in the period 1994–1997 for five sites (rural and urban) in the UK. Sousa et al. [41] examined MLR and ANN models to predict next-day hourly surface O<sub>3</sub> concentration values in Oporto (Northern Portugal). Capilla [42] used MLR and ANN models to predict surface O<sub>3</sub> for 1, 8, and 24 h in advance in an urban area of Valencia (Spain). Yu et al. [43] used MLR and ANN models to predict the maximum concentration of surface ozone. In all studies mentioned above, the ANN methods gave better results; however, in most cases, improvement was marginal.

In recent years, there have been many papers using more advanced machine learning methods. Freeman et al. [44] predicted an 8-h averaged concentration of surface O<sub>3</sub> using deep learning techniques such as Long Short-term Memory (LSTM) and Recurrent Neural Network (RNN). Ko et al. [45] forecasted the hourly concentration of surface O<sub>3</sub> for the upcoming 24 h using ANN and bidirectional LSTM models with a limited number of input data (surface O<sub>3</sub>, temperature, relative humidity, and height of the planetary boundary layer). Ouafou et al. [46] compared the results of parametric (the Least Absolute Shrinkage and Selection Operator (LASSO) and Saddle Point Least Squares (SPLS) method) and non-parametric (Bagging, Classification and Regression Trees (CART) and Random Forest (RF)) methods to forecast daily surface O<sub>3</sub> in Morocco. Jia et al. [47] used a sequence-to-sequence deep learning model to predict surface O<sub>3</sub> for the next 6 h over the Yangtze River Delta in China. Juarez et al. [48] employed eight machine learning ap-

proaches (linear regression, Support Vector Machines (SVM), K-Nearest Neighbors (KNN) algorithm, RF, Decision Trees, LSTM, AdaBoost, XGBoost) to forecast surface  $O_3$  for the next 24 h in Delhi.

The main objective of the work was a 24 h forecast of the hourly averaged surface  $O_3$  with steps every 3 h from 0:00 GMT for rural and suburban areas in Poland. We choose a simple statistical approach (MLR and ANN) that is adapted to the case with a limited number of predictors available for these locations. Two sets of predictors are examined, i.e., the meteorological data (temperature and relative humidity) plus an hour of the day, and the set comprising in addition also 1-day lagged surface  $O_3$ , and 3 h lagged temperature and relative humidity. Section 2 presents the observing sites, examined data, and models' details. Performances of all examined models are shown in Section 3. Discussion and conclusions are in Section 4.

## 2. Materials and Methods

### 2.1. Site Description

Concurrent measurements of surface  $O_3$  concentrations (ppb) and meteorological parameters: temperature ( $^{\circ}C$ ), and relative humidity (%) were carried out in the Belsk observatory and Racibórz observatory from September 2018 to September 2021 (Figure 1, Table 1).



**Figure 1.** Location of the stations considered in the study. (source: nationsonline.org).

**Table 1.** Characteristics of the stations.

Station Name	Altitude (m a.s.l.)	Latitude	Longitude	Station Type
Belsk	176	51.837 N	20.792 E	rural
Racibórz	193	50.083 N	18.192 E	suburban

The first measuring station, Belsk, represents rural background conditions. It is located in the central part of Poland in typical rural areas, 50 km south of Warsaw at the

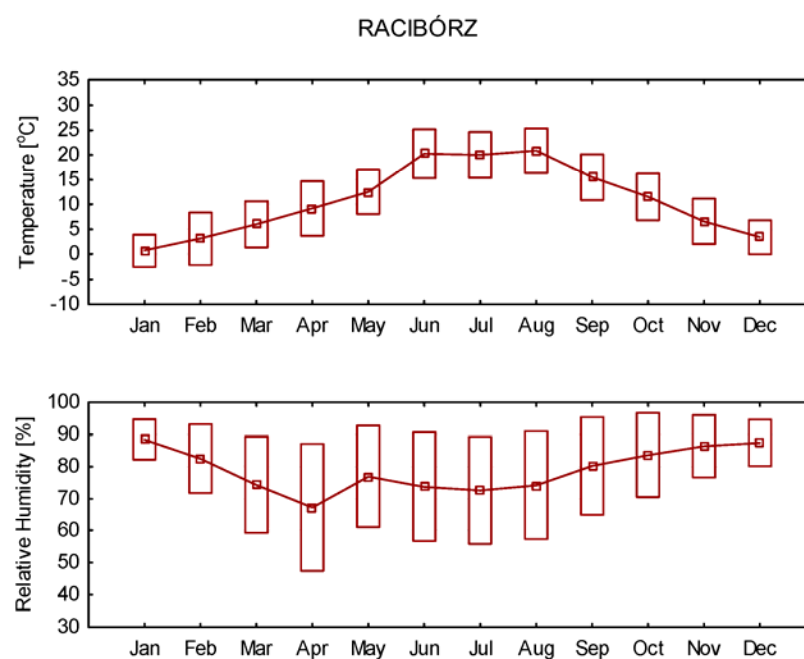
Central Geophysical Observatory Belsk. It is situated in the direct neighborhood of the Modrzewina nature reserve, far away from potential sources of anthropogenic pollution. The station is surrounded by coniferous forest and agricultural-horticultural lands. Belsk station is included in the National Air Quality Monitoring Network managed by the Main Inspectorate for Environmental Protection.

The second measuring station, Racibórz, represents suburban background conditions. It is located in the southern part of Poland, about 5 km from the Czech Republic border. It is situated on the southwestern outskirts of the city, in the immediate vicinity of single-family housing and agricultural areas from the west side and National Road No. 45 (about 150 m from the station) and typical urban infrastructure from the east site.

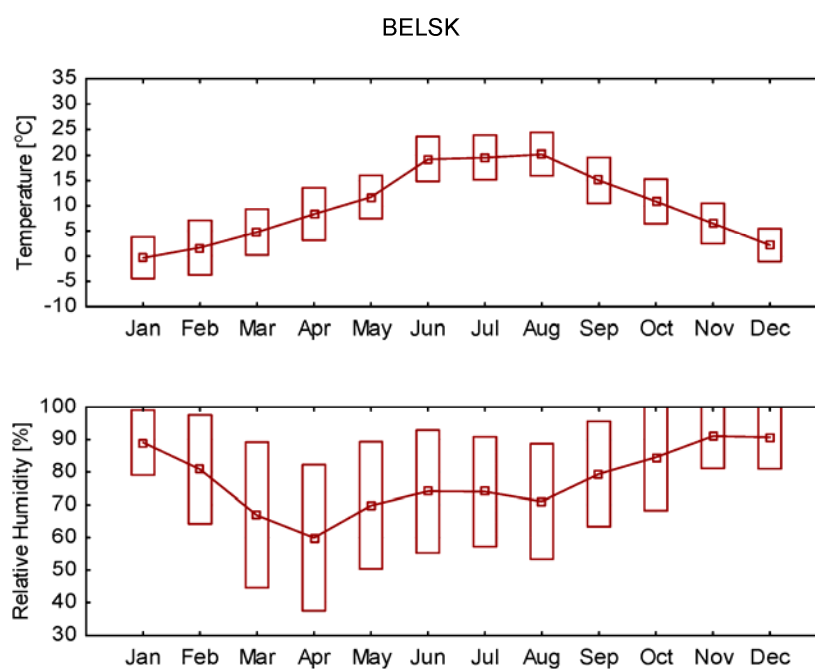
The selection of these locations, which represent rural and suburban conditions, makes it possible to conduct comparative statistical analysis for places with different chemical regimes.

## *2.2. Meteorological Conditions*

In this work, only two meteorological parameters are considered, including temperature [°C] and relative humidity [%]. The monthly variation of both parameters for Racibórz (a) and Belsk (b) stations are presented in Figure 2.



(a)



(b)

**Figure 2.** Monthly averaged values of temperature [°C] and relative humidity [%] in Racibórz (a) and Belsk (b) for the period 2018–2021. Points display the mean value; the box shows the range: mean  $\pm$  1 standard deviation.

At both locations, a characteristic annual cycle of temperature with a maximum during summer and a minimum during winter was noted. Generally, higher values of temperature were observed in Racibórz station. The differences for individual months ranged from 1.5 °C in February to 0.4 °C in November. The highest values of the monthly

mean temperature at both stations were noted in August (20.9 °C—Racibórz, and 20.2 °C—Belsk) while the lowest in January (0.7 °C—Racibórz and −0.3 °C—Belsk). The annual cycle of relative humidity is characterized by spring-summer minimum and winter maximum. The higher values for most of the year were recorded in Racibórz. The highest monthly mean relative humidity was observed in January (88%—Racibórz) and in November (91%—Belsk), while the lowest values were found in April (67%—Racibórz and 60%—Belsk).

### 2.3. Data Description

#### 2.3.1. Ground-Based Stations

Hourly-averaged meteorological parameters at Belsk were provided by the Department of Physics of the Atmosphere, Institute of Geophysics, Polish Academy of Sciences. Hourly-averaged surface O<sub>3</sub> concentrations were obtained from the Main Inspectorate for Environmental Protection. In Racibórz, measurements of meteorological parameters were performed by the Institute of Environmental Engineering of the Polish Academy of Sciences. The air pollution concentrations (including surface O<sub>3</sub>) were obtained from the Department of Physics of the Atmosphere, Institute of Geophysics, Polish Academy of Sciences.

Surface O<sub>3</sub> concentrations were monitored by Thermo Scientific 49i (Belsk) and Environment 42 (Racibórz) ozone analyzers, with the use of the UV absorption method and reference to the norm PN-EN 14625. In both stations, the surface O<sub>3</sub> monitors were regularly calibrated with a certified standard photometer and certified gas mixtures. Detailed checks of the surface O<sub>3</sub> data, i.e., verification and validation, as well as analysis of the deviations of the concentrations measured at nearby stations with the same category (rural or suburban), to ensure adequate data quality were performed. Meteorological parameters were measured using Vaisala Milos m520 and Lufft WS510-UMB (Belsk), and Meteo Davis Vantage Pro 2 (Racibórz). The 1 h averages of surface O<sub>3</sub> and meteorological parameters constitute the basis for further statistical calculations, which were done using the Statistica 12 package.

#### 2.3.2. CAMS

The Copernicus Atmosphere Monitoring Service (CAMS) is a service implemented by the European Center for Medium-Range Weather Forecasts (ECMWF) that provides continuous data and information on atmospheric composition. CAMS produces global forecasts for atmospheric composition twice a day. The initial conditions of each forecast are obtained by combining a previous forecast with current satellite observations through a process called data assimilation. This best estimate of the state of the atmosphere at the initial forecast time step called the analysis, provides estimates of the concentration of atmospheric pollutants at sites where no direct observations are available. Surface O<sub>3</sub> forecasts were downloaded from CAMS European air quality forecasts dataset. This dataset provides daily air quality analyses and forecasts for Europe.

CAMS produces specific daily air quality analyses for the European domain at high spatial resolution (0.1 degrees, approx. 10 km). In parallel, air quality forecasts are produced once a day for the next four days. Both the analysis and the forecast are available at hourly time steps at seven height levels, including the surface level. For this study, a set of the following air quality models were used: *Chimere*, *Emep*, *Ensemble*, *Mocage*, *Match*, *Lotos*, and *Euradim*. A detailed description of selected chemistry-transport models is available in Colette et al. [49].

### 2.4. Models

MLR and ANN (with multiple the perceptron (MLP) approach) were used to predict surface O<sub>3</sub> concentration using basic meteorological parameters (temperature and relative humidity) as explaining variables. Hour of the day and surface O<sub>3</sub> concentration in

the previous day (24 h back) was also attached to the input list. Time of the day can be a useful predictor, especially in urban environments where vehicular emissions are strongly dependent on the time of day [50]. Additionally, the most important meteorological predictors (e.g., temperature, solar radiation) are characterized by a distinct daily course with the maximum during noon hours and minimum during night. Predictors used in the models have a 3 h time resolution since 00:00 UTC. Both models were developed separately for Belsk and Racibórz for each season of the year: spring (March–April–May), summer (June–July–August), autumn (September–October–November), and winter (December–January–February). MLR and ANN models were chosen because they are tailored to the limited number of predictors available at the locations. These models can predict short-term surface ozone variability in many places equipped only with an ozone meter and a simple weather station.

#### 2.4.1. Multiple Regression Analysis

MLR is one of the most common tools used in surface  $O_3$  prediction. It is based on the relationship between the  $O_3$  concentration, and a set of predictors (usually including meteorological and chemical drivers) obtained by the least-squares method [51–53]. In this work, the forward stepwise regression method was used. It consists of the next (stepwise) adding a new variable included in the model to the predictor list, which at a given step has the most significant influence on the dependent variable.

#### 2.4.2. Artificial Neural Network

In recent years ANN, especially the MLP approach, has become an efficient alternative to traditional statistical techniques. A great advantage of ANN is the ability to model the highly non-linear relationships between predictors and predictand variables. The ANN system consists of a system of neurons interconnected by weights. The neurons are divided into input, hidden, and output layers. Using a training set consisting of series of input and related output data, it is possible to learn the network. During the process of learning, the training data are repeatedly presented to MLP, and weights are adjusted until the appropriate input-output matching is obtained and the resulting error of estimation is minimal. ANN is based on the non-linear transformation of input data to approximate output value. A comprehensive description of ANN is in Gardner and Dorling [54] and Spellman [39] and in the literature contained therein.

Comparative analysis of both methods could be helpful in indicating the dependency of the surface  $O_3$  concentration on selected explanatory variables. If the performance of the ANN model is comparable with the MLR model, it can be stated that the relationship between input and output variables is almost linear. When the performance of ANN outperforms MLR, it will indicate possible interactions between variables [40].

### 3. Results

#### 3.1. Diurnal and Seasonal Cycles of Surface $O_3$ Concentration

Surface  $O_3$  concentration in the suburban and rural regions has been analyzed statistically in terms of daily and annual variability in the period from September 2018 to September 2021. The box plots presented in Figure 3 summarize the hourly surface  $O_3$  variations in Racibórz and Belsk.

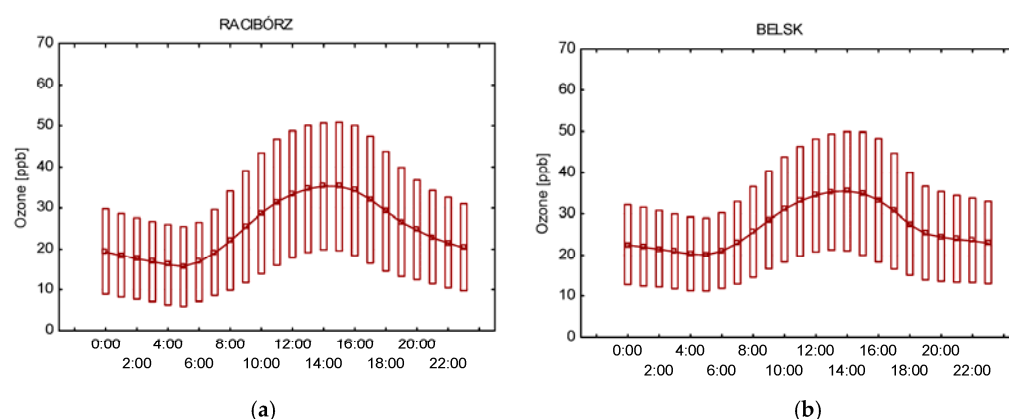


**Figure 3.** Mean daily course of surface O<sub>3</sub> from observations for the period from 2018 to 2021 in Racibórz (a) and at Belsk (b). The point shows the mean value, and the box displays the range: mean ± 1 standard deviation.

At both stations, a characteristic daily course of surface O<sub>3</sub> was recorded with maxima during the afternoon hours and minima in the early morning, just before sunrise. From 06:00, there was a constant increase in surface O<sub>3</sub> lasting until early afternoon (14:00), which is attributed to photochemical processes of ozone formation (involving VOC and NO<sub>x</sub> species) and vertical transport from upper layers of the atmosphere that develops during a day by convective activity in the atmospheric boundary layer [55]. Between 13:00 and 15:00, the highest values of surface O<sub>3</sub> were equal to 33.3 ppb and 34.5 ppb for Belsk and Racibórz, respectively. There has been a continuous slow decline since then until 05:00, when the daily minimum has been reached. Lowering surface O<sub>3</sub> levels during evening and night is attributed to the reduction of photochemical processes and processes of O<sub>3</sub> titration ( $\text{O}_3 + \text{NO} \rightarrow \text{NO}_2 + \text{O}_2$ ) [56,57].

The differences between rural and suburban surface O<sub>3</sub> are as follows:

- The average surface O<sub>3</sub> concentration is slightly higher at the rural station (25.1 ppb) than at the suburban (24.2 ppb). It is attributed to limited sinks of surface O<sub>3</sub> in rural areas (especially lower NO<sub>x</sub> level results in less surface O<sub>3</sub> destruction through titration processes).
- The cycle of diurnal variability of surface O<sub>3</sub> is weaker (has lower diurnal amplitude) at the rural station. The highest difference between surface O<sub>3</sub> concentration in Racibórz and Belsk was noted at 05:00 (~3.6 ppb). Lower concentrations in the suburban station during the night and morning hours are an indicator of the presence of fresh NO in urban areas [58]. Higher diurnal surface O<sub>3</sub> maxima also indicate a high concentration of surface O<sub>3</sub> precursors (NO<sub>x</sub>, VOC) at the site. The maximum of 1 h averaged surface O<sub>3</sub> concentration was equal to 91.2 ppb in Racibórz (19 June 2021) while 80.9 ppb at Belsk (1 July 2019).

Figure 4 presents the monthly averaged surface O<sub>3</sub> concentration at urban and rural stations. At both stations, a characteristic annual cycle with a spring-summer maximum and autumn minimum was recorded. The maximum was noted in April (38.3 ppb) at Belsk while in Racibórz in June (35.8 ppb). The existence of a maximum peak in April (Belsk) is probably related to the vertical transport of air from the upper atmosphere [59]. The existence of a broad spring-summer maximum (Racibórz) from April to August seems to be associated with the photochemical surface O<sub>3</sub> formation by processes involving NO<sub>x</sub> and VOC under the influence of solar radiation [43,50]. The annual minimum at each station was noted in November (~13 ppb).



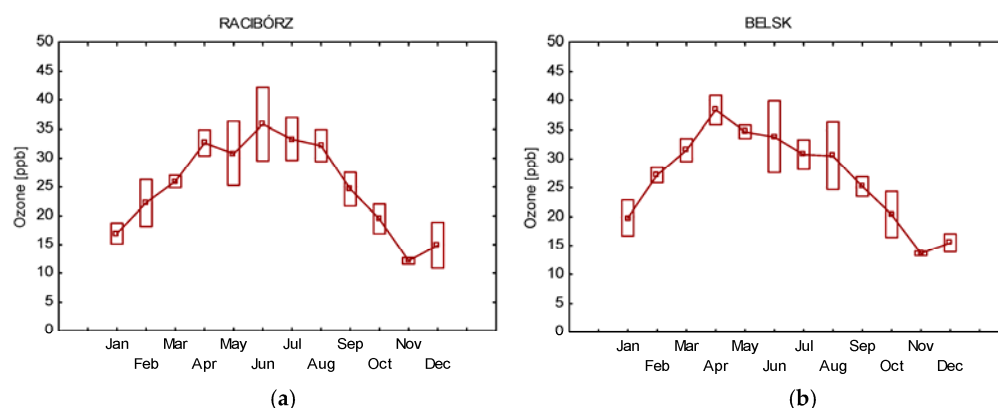


**Figure 4.** Monthly average surface O<sub>3</sub> concentrations in Racibórz (a) and at Belsk (b) for the period September 2018–September 2021. The point displays the mean value; the box shows the range: mean ± 1 standard deviation.

The rural-suburban surface O<sub>3</sub> differences were examined for individual hours and months. Results show that the differences (rural minus suburban) are much higher during night and morning hours (Figure 5a) and during winter-spring months (Figure 5b). During the afternoons and evenings (from 15:00 to 20:00), greater surface O<sub>3</sub> is noted in Racibórz station, similarly as during summer months (from June to August) which indicates the greater photochemical potential of surface O<sub>3</sub> formation.

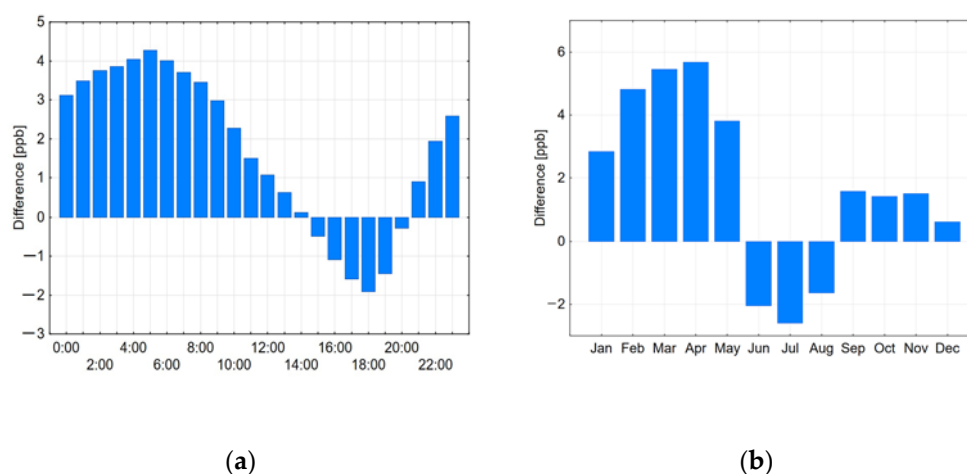


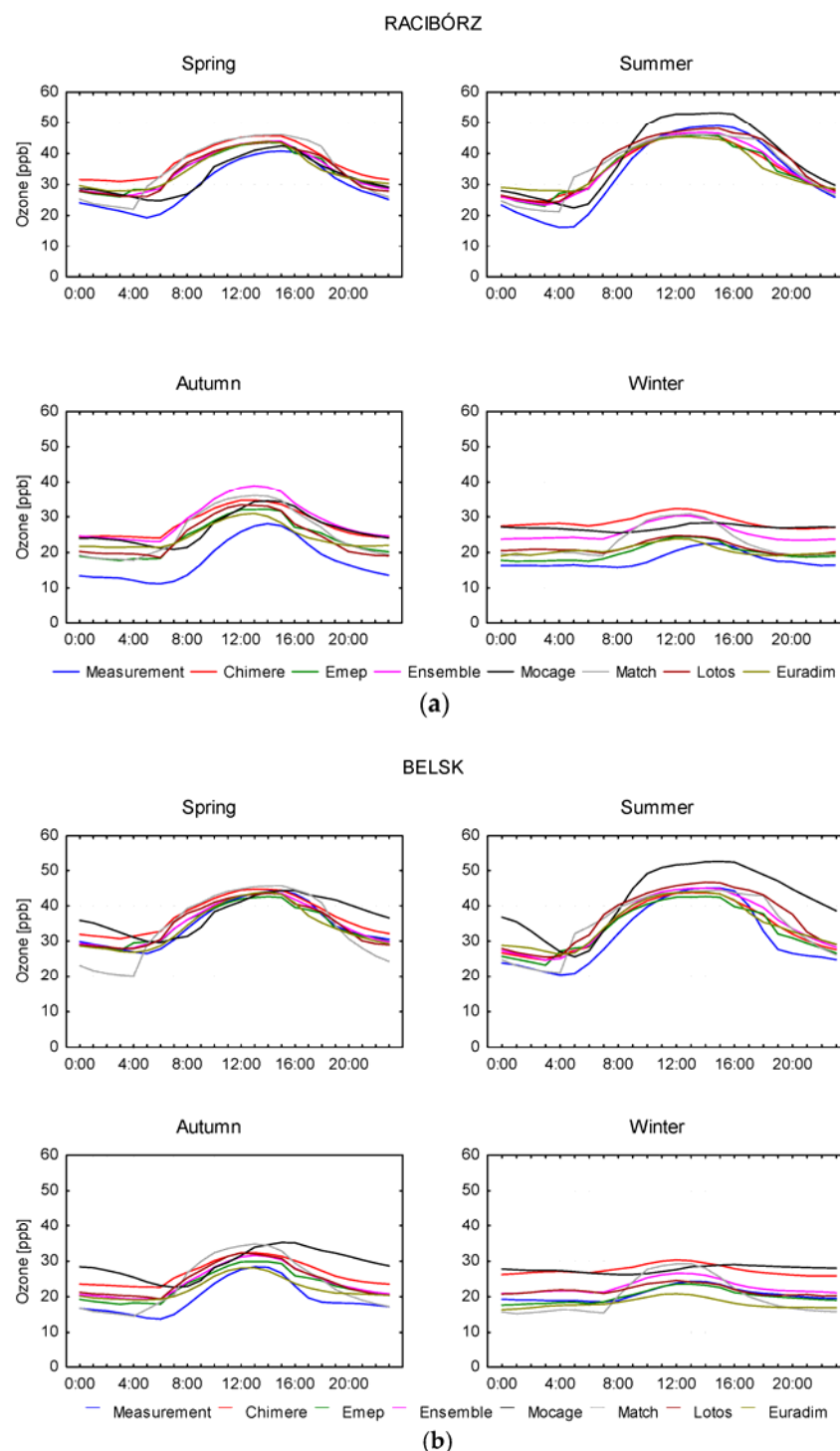
**Figure 5.** The differences between surface O<sub>3</sub> measured at Belsk and Racibórz (ppb), from 2018 to 2021, for diurnal (a) and monthly (b) scales.

The fit of the hourly and monthly surface O<sub>3</sub> values to a normal distribution was performed using the Shapiro-Wilk test (significance level:  $\alpha = 0.05$ ). The test was applied separately for all data from September 2018 to September 2021 separately for each hour during the day. The same test was performed for daily averaged values separately for each month (January–December) in the period 2018–2021. As the analyzed data were not normally distributed, the nonparametric U Mann-Whitney test was applied to find out whether the differences in surface O<sub>3</sub> concentrations between hours and months were statistically significant.

The difference between surface O<sub>3</sub> concentration in Belsk and Racibórz was statistically significant at a 95% confidence level for all hours, with the exception of hours between 13:00 and 16:00 and 20:00 and for months from January to May and for July.

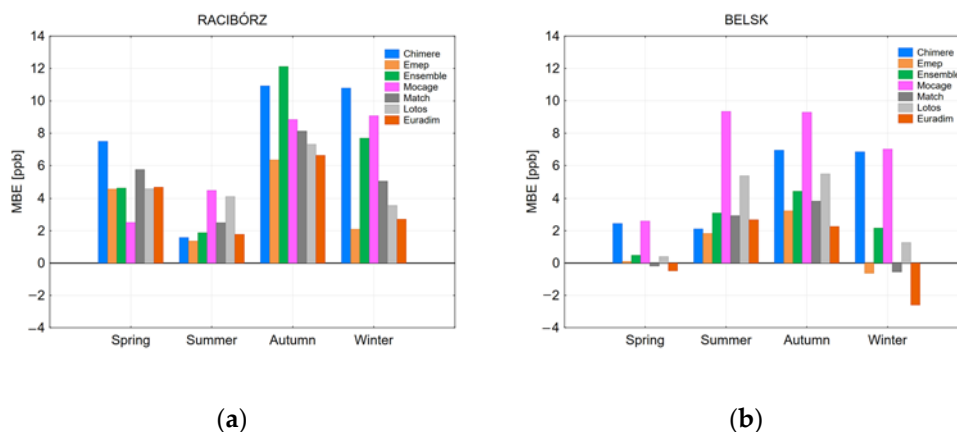
### 3.2. Seasonal Cycle of Surface O<sub>3</sub> Concentration from CAMS Simulations

Figure 6 presents averaged daily variations of surface O<sub>3</sub> from the measurements and CAMS forecasts for both stations for the period September 2018–September 2021. For each season, seven simulations: *Chimere*, *Emep*, *Ensemble*, *Mocage*, *Match*, *Lotos*, and *Euradim* were shown for both sites. Comparative analysis was performed separately for each location.



**Figure 6.** Time series of diurnal variation of surface O<sub>3</sub> concentration for each season at Racibórz (a) and Belsk (b) station for the period 2018–2021. Colors of lines: blue-measurement, red-*Chimere*, dark green-*Emep*, pink-*Ensemble*, black-*Mocage*, light grey-*Match*, brown-*Lotos*, light green-*Euradim*.

The mean differences between the CAMS forecasts and measured surface  $O_3$  are presented in Figure 7. All simulations show overestimation, especially during autumn and winter. In Belsk, the over- and under-estimations were slightly lower. Small under-estimations were noted during spring and winter for *Emep*, *Match*, and *Euradim* (up to 2.6 ppb). The simulations show differences not only in comparison with measurements but also when comparing CAMS pairs. More details on the CAMS-observation differences will be given in Section 3.3.



**Figure 7.** Mean bias error (see Equation (2) for definition), CAMS forecasts minus observed surface  $O_3$ , for the period 2018–2021, separately for each season for Racibórz (a) and Belsk (b) station.

In order to determine whether the differences between CAMS forecast, and observations were statistically significant, the non-parametric U Manna-Whitney test was performed. The test was carried out using all hourly averaged data for individual seasons from 2018 to 2021 for each location. In almost all cases (with the exception of the spring season at Belsk for *Emep*), the differences between CAMS forecasts and observed surface  $O_3$  data were statistically significant.

### 3.3. Quality of CAMS Forecasts

CAMS model performance is determined by standard measures of goodness of fit of the model to the measurements, including coefficient of determination ( $R^2$ ), mean bias error (MBE) [ppb], mean absolute error (MAE) [ppb], and root mean squared error (RMSE) [ppb] (Table 2). These measures (so-called comparative statistics) are given by Equations (1)–(4), respectively.

$$R^2 = \left( \frac{\frac{1}{n} \sum_{i=1}^n (x_i - \bar{x})(y_i - \bar{y})}{SD_x SD_y} \right)^2 \quad (1)$$

$$MBE = \frac{1}{n} \sum_{i=1}^n (y_i - x_i) \quad (2)$$

$$MAE = \frac{1}{n} \sum_{i=1}^n |y_i - x_i| \quad (3)$$

$$RMSE = \sqrt{\frac{1}{n} \sum_{i=1}^n (y_i - x_i)^2} \quad (4)$$

where:  $x_i$ —observed variable,  $y_i$ —predicted variable,  $\bar{x}$ —mean of  $x$  variable,  $\bar{y}$ —mean of  $y$  variable,  $SD_x$ —standard deviation of observed variable,  $SD_y$ —standard deviation of the predicted variable.

**Table 2.** Summary of comparative statistics of surface O<sub>3</sub> concentrations between measured and CAMS forecasts. MBE, MAE and RMSE are in ppb.

Index	Racibórz						Belsk							
	CH	EM	EN	MO	MA	LO	EU	CH	EM	EN	MO	MA	LO	EU
Spring														
R <sup>2</sup>	0.48	0.52	<b>0.54</b>	0.42	0.40	0.36	<b>0.22</b>	0.49	0.52	<b>0.57</b>	<b>0.24</b>	0.47	0.40	0.35
MBE	<b>7.49</b>	4.58	4.64	<b>2.52</b>	5.75	4.60	4.70	2.45	<b>0.10</b>	<b>0.49</b>	2.61	−0.18	0.41	−0.48
MAE	9.12	7.52	<b>7.29</b>	7.65	9.12	9.30	<b>9.39</b>	6.00	5.45	<b>5.01</b>	<b>7.84</b>	6.83	6.91	6.84
RMSE	11.46	9.63	<b>9.42</b>	9.83	11.59	11.77	<b>12.30</b>	7.71	7.18	<b>6.71</b>	<b>10.16</b>	8.69	9.03	8.99
Summer														
R <sup>2</sup>	0.61	0.53	<b>0.70</b>	0.61	0.56	0.56	<b>0.41</b>	0.54	0.42	<b>0.60</b>	<b>0.40</b>	0.49	0.45	0.41
MBE	1.58	<b>1.37</b>	1.89	<b>4.49</b>	2.50	4.12	1.78	2.12	<b>1.83</b>	3.10	<b>9.34</b>	2.93	5.36	2.69
MAE	8.04	8.66	<b>7.34</b>	8.76	8.49	8.80	<b>9.66</b>	7.02	7.62	<b>6.82</b>	<b>11.39</b>	7.65	8.85	8.11
RMSE	10.01	10.83	<b>9.21</b>	10.95	10.66	11.14	<b>12.12</b>	9.04	9.70	<b>8.84</b>	<b>14.25</b>	9.78	11.45	10.35
Autumn														
R <sup>2</sup>	0.49	<b>0.58</b>	0.40	0.46	0.53	0.46	<b>0.37</b>	0.55	0.63	<b>0.67</b>	<b>0.39</b>	0.55	0.49	0.52
MBE	10.93	<b>6.35</b>	<b>12.13</b>	8.84	8.12	7.32	6.63	6.95	3.23	4.45	<b>9.29</b>	3.83	5.47	<b>2.27</b>
MAE	11.58	<b>8.03</b>	<b>12.54</b>	9.99	9.62	9.98	9.12	8.35	<b>5.77</b>	6.11	<b>10.66</b>	6.82	8.00	6.16
RMSE	13.67	<b>10.01</b>	<b>16.18</b>	12.53	11.77	12.16	11.58	9.82	<b>7.29</b>	7.52	<b>12.81</b>	8.57	9.85	7.85
Winter														
R <sup>2</sup>	0.39	<b>0.51</b>	0.34	0.20	0.36	<b>0.23</b>	0.25	0.45	<b>0.58</b>	0.53	0.26	0.44	<b>0.22</b>	0.38
MBE	<b>10.79</b>	<b>2.10</b>	7.69	9.07	5.02	3.56	2.71	6.84	−0.62	2.17	<b>7.02</b>	<b>−0.54</b>	1.27	−2.60
MAE	<b>11.42</b>	<b>5.59</b>	9.01	10.46	8.02	9.33	7.29	8.12	<b>4.86</b>	5.42	<b>9.27</b>	6.27	8.40	6.43
RMSE	<b>13.54</b>	<b>7.36</b>	12.09	13.25	10.19	11.78	9.51	9.86	<b>6.30</b>	6.93	<b>11.56</b>	7.80	10.46	8.15

CH-Chimere, EM-Emepe, EN-Ensemble, MO-Mocage, MA-Match, LO-Lotos, EU-Euradim. For each station, the maximum value is denoted in bold, but the minimum is in bold italics.

The R<sup>2</sup> values show considerable variation depending on the season of the year. The highest values were found in summer and autumn, while the lowest were in winter. The R<sup>2</sup> values in Racibórz ranged from 0.22 (*Euradim*-spring) to 0.70 (*Ensemble*-summer). For Belsk, these values were correspondingly lower, ranging from 0.22 (*Lotos*-winter) to 0.67 (*Ensemble*-autumn). All R<sup>2</sup> values were statistically significant. The MBE values indicate a general tendency to overestimate observed values. The highest values were noted during autumn and winter. The MBE values in Racibórz varied between 1.37 ppb (*Emepe*-summer) and 12.13 ppb (*Ensemble*-autumn). Lower values of MBE were noted in Belsk and ranged from 0.10 ppb (*Emepe*-spring) to 9.34 (*Mocage*-summer). The MAE values in Racibórz ranged from 5.59 ppb (*Emepe*-winter) to 12.54 ppb (*Ensemble*-autumn). For Belsk, these values were correspondingly lower and ranged from 5.01 ppb (*Ensemble*-spring) to 14.25 ppb (*Mocage*-summer). The RMSE values in Racibórz varied from 7.36 ppb (*Emepe*-winter) to 16.18 ppb (*Ensemble*-autumn) while in Belsk from 6.30 ppb (*Emepe*-winter) to 14.25 ppb (*Mocage*-Summer). The higher RMSE values compared with MAE values were noted for each season and for both locations, which indicates an appearance of large residual values. Both MAE and RMSE show the better statistical performance of CAMS forecasts in spring (Belsk) and summer (Racibórz).

### 3.4. Performance of MLR and ANN Models

Various models for predicting surface O<sub>3</sub> are possible, ranging from the MLR model to sophisticated artificially intelligent ones such as XGBoost, based on many predictors containing chemical and weather components. Here we use two types of forecast model, i.e., MLR and ANN, which are adapted to a limited number of input variables available at the sites. The former aims to model the linear input-output relationship, and the latter one is to account for the possible nonlinearity effects between input variables and output.

Prediction of 1 h mean of surface O<sub>3</sub> every 3 h from 0:00 GMT for each season of the year was based on observed meteorological data measured (every 3 h) at the stations. Using Statistica 12, ANN package, the models were developed for 2 independent sets of input data. The former one consisted of the following predictors: the hour of the day, temperature [°C], and relative humidity [%]. The latter one additionally takes into account: temperature 3 h back, relative humidity 3 h back, and surface O<sub>3</sub> concentration 24 h back [ppb]. Particular data sets were implemented for the automatic network designer function. The input data set was divided into training (70%), test (15%), and validation (15%) subsets. Participants for each subset were selected randomly. Testing three-layer MLP with different functions of activation and different number of neurons in the hidden layer, the most appropriate topology of network structure was found. Table 3 presents the architecture of ANN for the validation subset used in the prediction.

**Table 3.** Structure of ANN networks selected for surface O<sub>3</sub> prediction.

Season	ANN Structure	Error Function	Activation Function (Hidden Layer)	Activation Function (Output Layer)
Racibórz				
Spring	3-5-1	BFGS	Tanh	Linear
	6-7-1	BFGS	Tanh	Linear
Summer	3-8-1	BFGS	Tanh	Exponential
	6-8-1	BFGS	Tanh	Linear
Autumn	3-10-1	BFGS	Tanh	Logistic
	6-4-1	BFGS	Logistic	Linear
Winter	3-8-1	BFGS	Logistic	Exponential
	6-7-1	BFGS	Tanh	Exponential
Belsk				
Spring	3-5-1	BFGS	Logistic	Exponential
	6-8-1	BFGS	Logistic	Logistic
Summer	3-8-1	BFGS	Exponential	Exponential
	6-7-1	BFGS	Exponential	Linear
Autumn	3-4-1	BFGS	Logistic	Linear
	6-10-1	BFGS	Exponential	Tanh
Winter	3-8-1	BFGS	Tanh	Tanh
	6-9-1	BFGS	Tanh	Tanh

Depending on the number of input data sets, the best architecture of ANN models consisted of 3 or 6 neurons in the input layer, from 4 to 10 in the hidden layer, and 1 neuron in the output layer. The models used the gradient quasi-Newton BFGS (Broyden-Fletcher-Goldfarb-Shanno) learning algorithm. The selection of the best networks was performed considering the same statistical measures (evaluative statistics) used for quality checking of the CAMS forecasts (see Table 2). Table 4 presents the values of evaluative statistics using MLR and ANN for both sets of input data, for each season of the year separately for Racibórz and Belsk stations. Both kinds of models were developed based on two sets of input data, including three predictors (hour of the day, temperature,

relative humidity) or six predictors (hour of the day, temperature, relative humidity, temperature 3 h back, relative humidity 3 h back, previous day's surface O<sub>3</sub> concentration). Performance indexes for ANN models were calculated for the validation data subset. The visual reference of results from Table 4, presenting the relative ranking of individual models, is shown in Figures 8–11.

**Table 4.** Comparative statistics for MLP and ANN models for validation subset (MLR 3 = multiple linear regression with an input data set consisting of three predictors, ANN 3 = artificial neural network with an input data set consisting of three predictors, MLR 6 = multiple linear regression with an input data set consisting of six predictors, ANN 6 = artificial neural network with an input data set consisting of three predictors). MBE, MAE and RMSE are in ppb.

Index	MLR3	ANN3	MLR6	ANN6	MLR3	ANN3	MLR6	ANN6
	Racibórz				Belsk			
Spring								
R <sup>2</sup>	0.52	0.54	0.62	0.66	0.58	0.67	0.64	0.70
MBE	0.04	−0.74	−0.01	−0.46	0.00	−0.31	−1.23	0.22
MAE	6.55	5.91	5.85	5.12	5.01	4.09	4.75	4.01
RMSE	8.38	7.72	7.49	6.61	6.31	5.24	6.04	5.18
Summer								
R <sup>2</sup>	0.71	0.77	0.78	0.81	0.65	0.71	0.71	0.73
MBE	−0.02	0.12	−0.02	−0.15	−0.16	−0.57	0.00	−0.43
MAE	6.62	5.49	5.68	5.08	5.76	5.31	5.32	5.21
RMSE	8.39	7.29	7.27	6.54	7.48	6.87	6.81	6.65
Autumn								
R <sup>2</sup>	0.65	0.65	0.68	0.69	0.68	0.71	0.68	0.75
MBE	−0.04	−0.10	−0.02	−0.09	0.03	0.69	0.02	0.69
MAE	5.64	5.41	5.30	5.18	4.75	4.26	4.52	4.07
RMSE	7.03	6.75	6.57	6.43	6.04	5.54	5.98	5.19
Winter								
R <sup>2</sup>	0.38	0.32	0.43	0.45	0.19	0.30	0.37	0.48
MBE	0.13	0.07	0.40	0.04	−0.16	−1.13	0.13	−0.68
MAE	6.48	6.34	5.94	5.84	6.96	6.74	6.00	5.86
RMSE	8.05	7.69	7.37	7.23	8.49	8.28	7.49	7.16

For each station, the maximum value is denoted in bold, but the minimum is in bold italics.

MLR model that was trained by a set of three input data (MLR3) explains up to 71% of the variance in surface O<sub>3</sub> in Racibórz (summer) and up to 68% at Belsk (autumn). In turn, the ANN models trained by the same set of input data (ANN3) explains up to 77% in Racibórz (summer) and up to 71% at Belsk (summer and autumn). The use of a larger set of six input data results in improved model performance. The MLR6 model explains up to 78% in Racibórz and up to 71% at Belsk, while the ANN6 model explains up to 81% in Racibórz and up to 75% at Belsk. Generally, high R<sup>2</sup> values are for summer and autumn but the lowest for winter. It's worth noting that during summer, distinctly higher R<sup>2</sup> values were noted for Racibórz station. During other seasons the R<sup>2</sup> values between both stations were comparable.

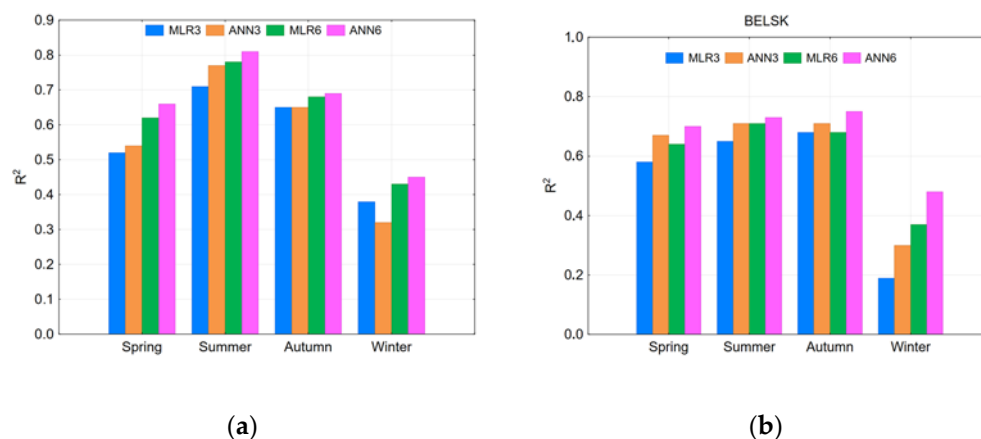


**Figure 8.** Coefficient of determination ( $R^2$ ) for Racibórz (a) and Belsk (b) by model and season. MLR3—MLR based on a set of 3 input data, ANN3—ANN based on a set of 3 input data, MLR6—MLR based on a set of 6 input data, ANN6—ANN based on a set of 6 input data.

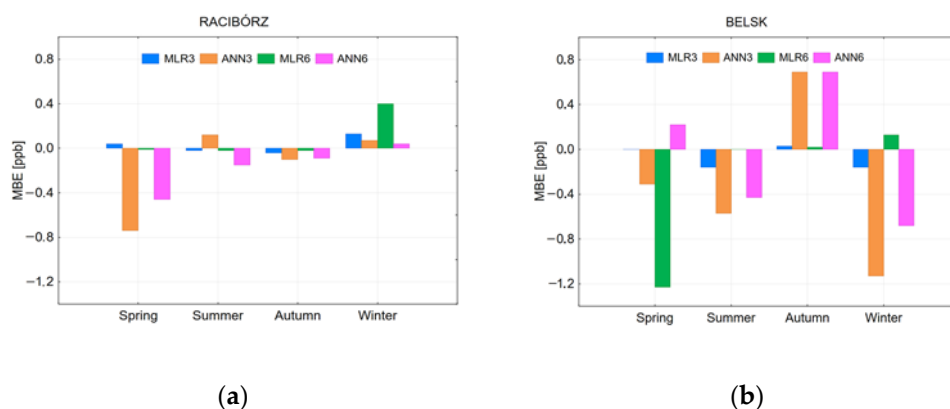


**Figure 9.** The same as Figure 8 but for mean bias error (MBE) for Racibórz (a) and Belsk (b).

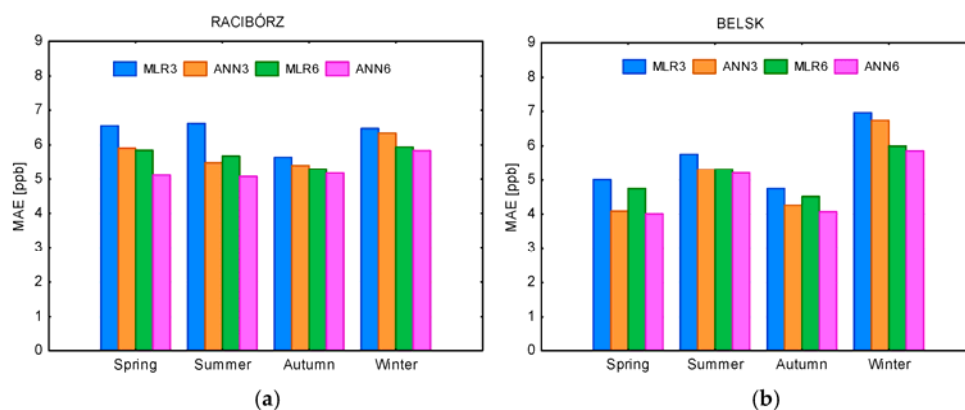


**Figure 10.** The same as Figure 8 but for mean absolute error (MAE) for Racibórz (a) and Belsk (b).

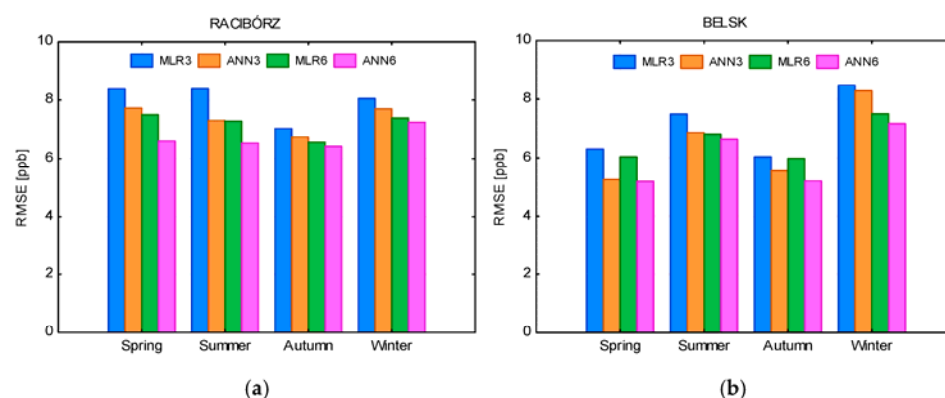


**Figure 11.** The same as Figure 8 but for root mean square error (RMSE) for Racibórz (a) and Belsk (b).

The MBE values are small, ranging between  $-0.74$  ppb (ANN3-spring) and  $0.40$  ppb (MLR6-winter) in Racibórz and between  $-1.23$  ppb (MLR6-winter) and  $0.69$  ppb (ANN3-autumn) at Belsk. It shows great variation depending on the season and the kind of models. All models tend to slightly overestimate surface  $O_3$  concentrations. When comparing stations, higher absolute values of MBE were noted in Belsk.

Analyzing MLR3 models, the MAE value ranged between  $5.64$  ppb (autumn) and  $6.62$  ppb (summer) in Racibórz and between  $4.75$  ppb (autumn) and  $6.96$  ppb (winter) at Belsk. For ANN3 models, the MAE value ranged from  $5.41$  ppb (autumn) to  $6.34$  ppb (winter) in Racibórz and from  $4.09$  ppb (spring) to  $6.74$  ppb (winter) at Belsk. Addition of lagged ozone data and two lagged meteorological predictors reduced the MAE value by MLR6 models to  $5.30$  ppb (autumn) in Racibórz and to  $4.52$  ppb (autumn) at Belsk and of ANN6 models to  $5.08$  ppb (summer) in Racibórz and to  $4.01$  ppb (spring) at Belsk. For both models, the highest MAEs were noted for the winter months.

The results of RMSE follow a similar pattern to MAE, although its value in all cases is slightly higher than MAE because of higher sensitivity to outliers. For MLR3 models, trained with a set of three input data, RMSE ranged between  $7.03$  ppb (autumn) and  $8.39$  ppb (summer) in Racibórz and between  $6.04$  ppb (spring) and  $8.49$  ppb (winter) at Belsk. ANN3 models perform slightly better with RMSE between  $6.75$  ppb (autumn) and  $7.69$  ppb (winter) in Racibórz and between  $5.24$  ppb (spring) and  $8.28$  ppb (winter) in Belsk. Minimum RMSE for MLR6 models (trained with a set of 6 input data) were equal to  $6.57$  ppb (autumn) in Racibórz and  $5.98$  ppb (autumn) in Belsk. RMSE for ANN6 models reduced to  $6.43$  ppb (autumn) in Racibórz and to  $5.18$  ppb (spring) at Belsk.

Comparing model performance in terms of the number of input data (three or six), it appears that ANN, in all cases, is somewhat better than MLR. It seems that the inherent element of nonlinearity in ANN models provides a more accurate surface  $O_3$  forecast compared with MLR. The inclusion of additional input data, e.g., lagged surface  $O_3$  values (24 h back) and meteorological variables (temperature and relative humidity 3 h back), resulted in better performance of both kinds of models. However, improvement is slightly better for MLR than for ANN models.

### 3.5. Comparison of Performance of MLR and ANN with CAMS Simulations

The architecture of the MLR and ANN model was built using the meteorological variable measured in stations. Figures 12–15 present the results of the best CAMS forecast (blue), ANN3 (orange), and ANN6 (green) in terms of  $R^2$ , MBE, MAE, and RMSE for Racibórz and Belsk stations. Depending on the season, the best CAMS forecast was: *Emep* (50% of cases), *Ensemble* (40%), *Mocage* (3.3%), *Match* (3.3%), and *Euradim* (3.3%).



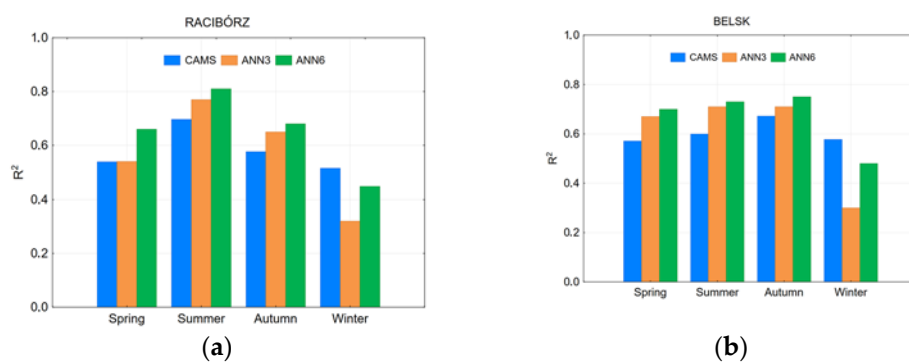


**Figure 12.**  $R^2$  for the best CAMS forecast, ANN3 and ANN6 for Racibórz (a) and Belsk (b).

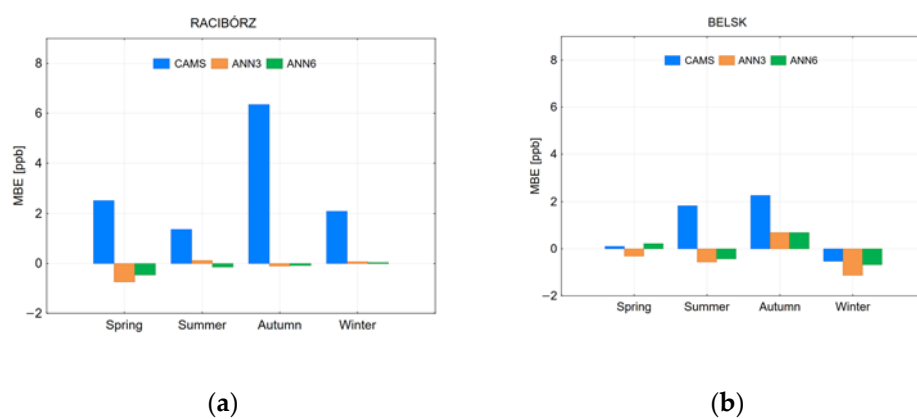


**Figure 13.** MBE for the best CAMS forecast, ANN3 and ANN6 for Racibórz (a) and Belsk (b).

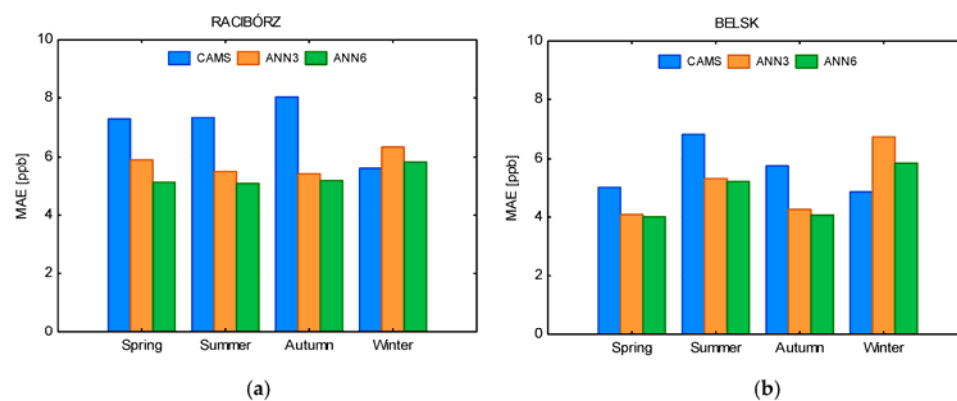


**Figure 14.** MAE for the best CAMS forecast, ANN3 and ANN6 for Racibórz (a) and Belsk (b).

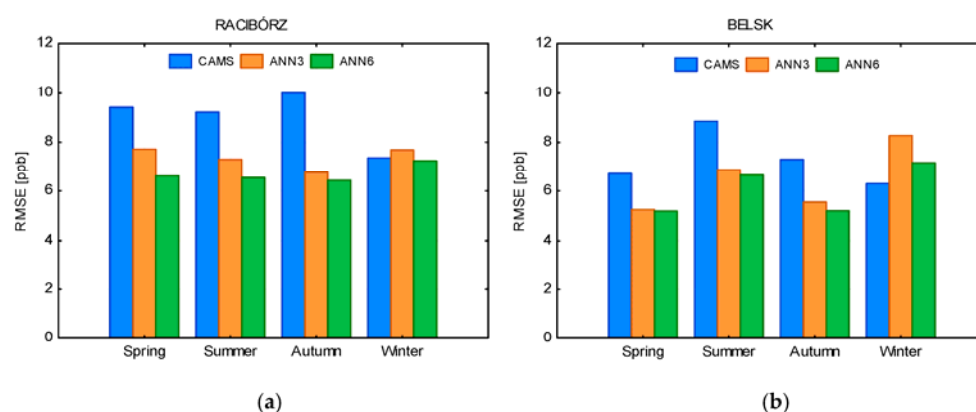


**Figure 15.** RMSE for the best CAMS forecast, ANN3 and ANN6 for Racibórz (a) and Belsk (b).

Comparing the performance of these three models in terms of  $R^2$  value, it can be stated that for spring, summer, and autumn, the  $R^2$  was higher for ANN3 and ANN6 models, while for winter, the CAMS simulation (*Emep*) was better. MBE values indicate the over-estimation by CAMS simulations for both locations during all seasons, with the exception of winter at Belsk, when small (below 1 ppb) under-estimation by *Match* forecast was recorded. In terms of MAE and RMSE, for spring, summer, and autumn, the forecast by ANN3 and ANN6 were better than those taken from the best CAMS forecast. In the winter season, the CAMS forecast reached a better fit for the measured data. It suggests that ANN with the MLP structure could be an effective tool supporting the prediction of surface  $O_3$  during spring-summer-autumn when there is a real risk of episodes of high surface  $O_3$ .

#### 4. Discussion

This study presents the performance of MLR and ANN (with an MLP approach) in forecasting surface  $O_3$  in rural and suburban locations in Poland. Both models were built using two separate sets of input data containing a limited number (three or six) of predictors. Because surface  $O_3$  is mainly formed by photochemical reactions, the combination of basic meteorological parameters (temperature and relative humidity) with additional variables, including an hour of the day and lagged surface  $O_3$  data, were used as an explanatory variable. Similarly, to Yi and Prybutok [37], Comrie [38], Spellmann [39], Gardner and Dorling [40], Sousa et al. [41], and Yu et al. [43], the results showed that the use of ANN models performs better than linear models what indicate possible interactions and non-linear relationships between predictors and surface  $O_3$ . MLR explained up to 78% of the variance in surface  $O_3$  in Racibórz and up to 71% in Belsk, while the ANN model explained up to 81% in Racibórz and up to 75% at Belsk.

The use of three additional input data, including the surface  $O_3$  concentration from the previous day, improves the quality of the estimation of both models. The gain is up to 18 percentage points for MLR and up to 13 percentage points for ANN models). It is worth noting that statistical models presented in this work used only the basic set of parameters determining surface  $O_3$  formation. Other meteorological parameters or in-situ surface  $O_3$  precursor concentrations ( $NO_x$ , VOC) were not included in the presented analysis. We can suggest that the inclusion of these predictors into a set of input data might further improve the results of modeling. MLR and ANN models provided better forecasts for the rural station (Belsk). It is probably related to the greater uniformity and representativeness of non-urban areas.

Surface  $O_3$  forecasts using ANN models were also performed based on CAMS meteorological data. The  $R^2$  values ranged up to 0.61 in Racibórz (summer) and up to 0.52 in Belsk (autumn), while RMSE values ranged up to 10.35 ppb in both locations. These results, in most cases, were better compared to results obtained by CAMS surface  $O_3$  fore-

casts but worse when compared with results obtained using measured meteorological data ( $R^2$  up to 0.81, RMSE up to 6.43 in Racibórz and  $R^2$  up to 0.75 and RMSE up to 5.18 ppb in Belsk). The performance of statistical models depends crucially on the quality of the forecast of the meteorological field. Using observed parameters is equivalent to using the perfect meteorological forecast.

Furthermore, this study investigates the efficiency of surface  $O_3$  prediction obtained by selected CAMS simulations. Statistical analysis of differences between measurements and CAMS forecasts showed significant overestimations of CAMS results, especially for Racibórz during the autumn season. Comparative analysis indicates better performance of MLR and ANN models trained by a set of six input data compared to CAMS simulations for both locations for all seasons with the exception of winter. Forecasts by MLR and ANN for the cold part of the year are less accurate, with an  $R^2$  value below 0.5 for both models. It is worth noticing that ANN, with three predictors (temperature, relative humidity, and the hour of the day) provided an even better forecast (except winter) than the best CAMS forecast. Such a simple forecast can be used for any place in Poland, and measurements of surface  $O_3$  are not necessary for the such forecast.

The results of the machine learning algorithm using different categories of predictors (including CAMS surface  $O_3$  simulations) for predicting surface  $O_3$  in Munich (Germany) were presented in the work of Balamurugan et al. [60]. In contrast to the present study, the results concerned the diurnal maximum (from 13:00 to 14:00) of surface  $O_3$  for the whole year without division into seasons. The Extreme Gradient Boosting (XGBoost) approach trained only on meteorology parameters (temperature, relative humidity, boundary layer height, wind speed, and wind direction) explained 77% of the variance of measured surface  $O_3$  with RMSE value  $\sim 8$  ppb. These results are comparable with MLR6 and ANN3 achieved in the present study. XGBoost trained only on CAMS data showed worse performance. It explained 75% of the variance in surface  $O_3$  with RMSE  $\sim 8.5$  ppb. The results obtained for the best CAMS simulations in the present study explained up to 70% of the variance in surface  $O_3$  with RMSE equal to 9.21 ppb (Racibórz—Summer). It is worth noticing that the performance of our statistical models in all seasons except winter was clearly better than CAMS alternatives (see Figures 11–14). Balamurugan et al. [60] found that the differences between  $R^2$  and RMSE for their models based on meteorology and CAMS  $O_3$  forecasts were rather marginal.

## 5. Conclusions

Surface ozone has been measured in the Polish national network involving monitoring of other gaseous components important for the determination of air quality. This study shows that effective forecasting of surface ozone for rural and suburban sites in Poland is possible using only surface  $O_3$ , temperature, and humidity. Monitoring of these weather variables can be carried out even by simplified weather stations, i.e., with no wind measurements. This low-cost configuration increases the number of locations providing short-term surface  $O_3$  predictions important to local communities.

**Author Contributions:** Conceptualization, I.P. and A.F.; methodology, I.P. and A.F.; preparation of data, J.J., A.P., K.K., and A.F.; statistical analysis; I.P.; writing—original draft preparation, I.P. and A.F.; writing—review and editing, A.P. and J.J.; preparation of figures, I.P.; supervision, A.P. and J.J. All authors have read and agreed to the published version of the manuscript.

**Funding:** This work was funded by the National Science Center in Poland under grant UMO-2017/25/B/ST10/01650. This work was partially founded by the Chief Inspectorate of Environmental Protection, GIOŚ/19/2021/DMS/NFOŚ. Observatory activities at Belsk and Racibórz were supported by Polish Ministry of Education and Science (Decision No. 13/E-41/SPUB/SP/2020).

**Institutional Review Board Statement:** Not applicable.

**Informed Consent Statement:** Not applicable.

**Data Availability Statement:** The observed surface O<sub>3</sub> from Racibórz and Belsk data is available on the IG PAS Data Portal (<https://dataportal.igf.edu.pl/organization/atmospheric-physics>) (accessed on 25 March 2023). The surface O<sub>3</sub> CAMS data is available through the website <https://ads.atmosphere.copernicus.eu/cdsapp#!/dataset/cams-europe-air-quality-forecasts?tab=form> (accessed on 25 March 2023). The temperature and relative humidity CAMS data are available through the website <https://ads.atmosphere.copernicus.eu/cdsapp#!/dataset/cams-global-atmospheric-composition-forecasts?tab=form> (accessed on 25 March 2023).

**Conflicts of Interest:** The authors declare no conflict of interest.

## References

- Ramsey, N.R.; Klein, P.M.; Moore, B. The Impact of Meteorological Parameters on Urban Air Quality. *Atmos. Environ.* **2014**, *86*, 58–67. <https://doi.org/10.1016/j.atmosenv.2013.12.006>.
- Crutzen, P. *A Discussion of the Chemistry of Some Minor Constituents in the Stratosphere and Troposphere*; Birkhuser Verlag: Basel, Switzerland, Pure and Applied Geophysics, 1973; Volume 106.
- Seinfeld, J.H. Urban Air Pollution: State of the Science. *Science* **1989**, *243*, 745–752. <https://doi.org/10.1126/science.243.4892.745>.
- Jacob, D.J. Heterogeneous Chemistry and Tropospheric Ozone. *Atmos. Environ.* **2000**, *34*, 2131–2159.
- Edwin, F. Danielsen Stratospheric-Tropospheric Exchange Based on Radioactivity, Ozone and Potential Vorticity. *J. Atmos. Sci.* **1968**, *25*, 502–518.
- Stohl, A. Stratosphere-Troposphere Exchange: A Review, and What We Have Learned from STACCATO. *J. Geophys. Res.* **2003**, *108*, 8516. <https://doi.org/10.1029/2002JD002490>.
- Hov, Ö.; Hesstvedt, E.; Isaksen, I.S.A. Long-Range Transport of Tropospheric Ozone. *Nature* **1978**, *273*, 341–344. <https://doi.org/10.1038/273341a0>.
- Gosten, H.; Heinrich, N.; Monnich, E.; Sprung, D.; Weppner, J.; Bakr Ramadan, A.; M Ezz El-din, M.R.; Ahmed, D.M.; Y Hassan, G.K. ON-line measurements of ozone surface fluxes: Part II. surface-level ozone fluxes onto the sahara desert. *Atmos. Environ.* **1996**, *30*, 911–918.
- Atkinson, R. Atmospheric Chemistry of VOCs and NOx. *Atmos. Environ.* **2000**, *34*, 2063–2101. [https://doi.org/10.1016/S1352-2310\(99\)00460-4](https://doi.org/10.1016/S1352-2310(99)00460-4).
- Sillman, S. The Relation between Ozone, NOx and Hydrocarbons in Urban and Polluted Rural Environments. *Atmos. Environ.* **1999**, *33*, 1821–1845.
- Dueñas, C.; Fernández, M.C.; Cañete, S.; Carretero, J.; Liger, E. Analyses of Ozone in Urban and Rural Sites in Málaga (Spain). *Chemosphere* **2004**, *56*, 631–639. <https://doi.org/10.1016/j.chemosphere.2004.04.013>.
- Han, J.; Kim, H.; Lee, M.; Kim, S.; Kim, S. Photochemical Air Pollution of Seoul in the Last Three Decades. *J. Korean Soc. Atmos. Environ.* **2013**, *29*, 390–406. <https://doi.org/10.5572/KOSAE.2013.29.4.390>.
- Pawlak, I.; Jarosławski, J. The Influence of Selected Meteorological Parameters on the Concentration of Surface Ozone in the Central Region of Poland. *Atmosphere-Ocean* **2015**, *53*, 126–139. <https://doi.org/10.1080/07055900.2014.969189>.
- Crutzen, P.J.; Zimmermann, P.H. The Changing Photochemistry of the Troposphere. *Tellus A* **1991**, *43*, 136–151. <https://doi.org/10.1034/j.1600-0870.1991.00012.x>.
- Forster, P.; Alterskjaer, K.; Smith, C.; Colman, R.; Damon Matthews, H.; Ramaswamy, V.; Storelvmo, T.; Armour, K.; Collins, W.; Dufresne, J.; et al. *SPM 923 7 Coordinating Lead Authors: Contributing Authors: Review Editors: Chapter Scientists: The Earth's Energy Budget, Climate Feedbacks and Climate Sensitivity*; Cambridge University Press: Cambridge, UK; New York, NY, USA, 2021pp. 923–1054. doi:10.1017/9781009157896.009.
- Sillman, S. Tropospheric Ozone and Photochemical Smog. In *Treatise on Geochemistry*; Elsevier: Amsterdam, The Netherlands, 2003; pp. 407–431.
- Malley, C.S.; Heal, M.R.; Mills, G.; Braban, C.F. Trends and Drivers of Ozone Human Health and Vegetation Impact Metrics from UK EMEP Supersite Measurements (1990–2013). *Atmos. Chem. Phys.* **2015**, *15*, 4025–4042. <https://doi.org/10.5194/acp-15-4025-2015>.
- Liu, X.; Tai, A.P.K.; Fung, K.M. Responses of Surface Ozone to Future Agricultural Ammonia Emissions and Subsequent Nitrogen Deposition through Terrestrial Ecosystem Changes. *Atmos. Chem. Phys.* **2021**, *21*, 17743–17758. <https://doi.org/10.5194/acp-21-17743-2021>.
- Wilson, A.; Rappold, A.G.; Neas, L.M.; Reich, B.J. Modeling the Effect of Temperature on Ozone-Related Mortality. *Ann. Appl. Stat.* **2014**, *8*, 1728–1749. <https://doi.org/10.1214/14-AOAS754>.
- Logan, J.A. Tropospheric Ozone: Seasonal Behavior, Trends, and Anthropogenic Influence. *J. Geophys. Res. Atmos.* **1985**, *90*, 10463–10482. <https://doi.org/10.1029/JD090iD06p10463>.
- Seinfeld, J.H.; Pandis, S.N. *Atmospheric Chemistry and Physics: From Air Pollution to Climate Change*, 2nd ed.; John Wiley & Sons: New York, NY, USA, 2006.
- Sillman, S.; Samson, P.J. Impact of Temperature on Oxidant Photochemistry in Urban, Polluted Rural and Remote Environments. *J. Geophys. Res.* **1995**, *100*, 11497. <https://doi.org/10.1029/94JD02146>.
- Arya, S.P. *Air Pollution Meteorology and Dispersion*; Oxford University Press: Oxford, UK, 1999.

24. Lelieveld, J.; Crutzen, P.J. The Role of Clouds in Tropospheric Photochemistry. *J. Atmos. Chem.* **1991**, *12*, 229–267. <https://doi.org/10.1007/BF00048075>.
25. Zhang, L.; Brook, J.R.; Vet, R. A Revised Parameterization for Gaseous Dry Deposition in Air-Quality Models. *Atmos. Chem. Phys.* **2003**, *3*, 2067–2082. <https://doi.org/10.5194/acp-3-2067-2003>.
26. Hodnebrog, Ø.; Solberg, S.; Stordal, F.; Svendby, T.M.; Simpson, D.; Gauss, M.; Hilboll, A.; Pfister, G.G.; Turquety, S.; Richter, A.; et al. Impact of Forest Fires, Biogenic Emissions and High Temperatures on the Elevated Eastern Mediterranean Ozone Levels during the Hot Summer of 2007. *Atmos. Chem. Phys.* **2012**, *12*, 8727–8750. <https://doi.org/10.5194/acp-12-8727-2012>.
27. Derwent, R.G.; Jenkin, M.E.; Saunders, S.M.; Pilling, M.J. Photochemical ozone creation potentials for organic compounds in northwest Europe calculated with a master chemical mechanism. *Atmos. Environ.* **1998**, *32*, 2429–2441.
28. Tarasova, O.A.; Karpetchko, A.Y. Accounting for Local Meteorological Effects in the Ozone Time-Series of Lovozero (Kola Peninsula). *Atmos. Chem. Phys.* **2003**, *3*, 941–949. <https://doi.org/10.5194/acp-3-941-2003>.
29. Camalier, L.; Cox, W.; Dolwick, P. The Effects of Meteorology on Ozone in Urban Areas and Their Use in Assessing Ozone Trends. *Atmos. Environ.* **2007**, *41*, 7127–7137. <https://doi.org/10.1016/j.atmosenv.2007.04.061>.
30. Vautard, R.; Beekmann, M.; Roux, J.; Gombert, D. Validation of a Hybrid Forecasting System for the Ozone Concentrations over the Paris Area. *Atmos. Environ.* **2001**, *35*, 2449–2461.
31. Vautard, R.; Moran, M.D.; Solazzo, E.; Gilliam, R.C.; Matthias, V.; Bianconi, R.; Chemel, C.; Ferreira, J.; Geyer, B.; Hansen, A.B.; et al. Evaluation of the Meteorological Forcing Used for the Air Quality Model Evaluation International Initiative (AQMEII) Air Quality Simulations. *Atmos. Environ.* **2012**, *53*, 15–37. <https://doi.org/10.1016/j.atmosenv.2011.10.065>.
32. Verma, N.; Lakhani, A.; Maharaj Kumari, K. High Ozone Episodes at a Semi-Urban Site in India: Photochemical Generation and Transport. *Atmos. Res.* **2017**, *197*, 232–243. <https://doi.org/10.1016/j.atmosres.2017.07.014>.
33. Lou, S.; Liao, H.; Yang, Y.; Mu, Q. Simulation of the Interannual Variations of Tropospheric Ozone over China: Roles of Variations in Meteorological Parameters and Anthropogenic Emissions. *Atmos. Environ.* **2015**, *122*, 839–851. <https://doi.org/10.1016/j.atmosenv.2015.08.081>.
34. Hu, J.; Chen, J.; Ying, Q.; Zhang, H. One-Year Simulation of Ozone and Particulate Matter in China Using WRF/CMAQ Modeling System. *Atmos. Chem. Phys.* **2016**, *16*, 10333–10350. <https://doi.org/10.5194/acp-16-10333-2016>.
35. Singh, J.; Singh, N.; Ojha, N.; Sharma, A.; Pozzer, A.; Kiran Kumar, N.; Rajeev, K.; Gunthe, S.S.; Rao Kotamarthi, V. Effects of Spatial Resolution on WRF v3.8.1 Simulated Meteorology over the Central Himalaya. *Geosci. Model Dev.* **2021**, *14*, 1427–1443. <https://doi.org/10.5194/gmd-14-1427-2021>.
36. Sharma, A.; Ojha, N.; Pozzer, A.; Mar, K.A.; Beig, G.; Lelieveld, J.; Gunthe, S.S. WRF-Chem Simulated Surface Ozone over South Asia during the Pre-Monsoon: Effects of Emission Inventories and Chemical Mechanisms. *Atmos. Chem. Phys.* **2017**, *17*, 14393–14413. <https://doi.org/10.5194/acp-17-14393-2017>.
37. Yi, J.; Prybutok, V.R. A neural network model forecasting for prediction of daily maximum ozone concentration in an industrialized urban area. *Environ. Pollut.* **1996**, *92*, 349–357.
38. Comrie, A.C. Comparing Neural Networks and Regression Models for Ozone Forecasting. *J. Air Waste Manag. Assoc.* **1997**, *47*, 653–663. <https://doi.org/10.1080/10473289.1997.10463925>.
39. Spellman, G. An Application of Artificial Neural Networks to the Prediction of Surface Ozone Concentrations in the United Kingdom. *Appl. Geogr.* **1999**, *19*, 123–136.
40. Gardner, M.W.; Dorling, S.R. Statistical Surface Ozone Models: An Improved Methodology to Account for Non-Linear Behaviour. *Atmos. Environ.* **2000**, *34*, 21–34.
41. Sousa, S.I.V.; Martins, F.G.; Alvim-Ferraz, M.C.M.; Pereira, M.C. Multiple Linear Regression and Artificial Neural Networks Based on Principal Components to Predict Ozone Concentrations. *Environ. Model. Softw.* **2007**, *22*, 97–103. <https://doi.org/10.1016/j.envsoft.2005.12.002>.
42. Capilla, C. Prediction of Hourly Ozone Concentrations with Multiple Regression and Multilayer Perceptron Models. *Int. J. Sustain. Dev. Plan.* **2016**, *11*, 558–565. <https://doi.org/10.2495/SDP-V11-N4-558-565>.
43. Yu, J.; Xu, L.; Gao, S.; Chen, L.; Sun, Y.; Mao, J.; Zhang, H. Establishment of a Combined Model for Ozone Concentration Simulation with Stepwise Regression Analysis and Artificial Neural Network. *Atmosphere* **2022**, *13*, 1371. <https://doi.org/10.3390/atmos13091371>.
44. Freeman, B.S.; Taylor, G.; Gharabaghi, B.; Thé, J. Forecasting Air Quality Time Series Using Deep Learning. *J. Air Waste Manag. Assoc.* **2018**, *68*, 866–886. <https://doi.org/10.1080/10962247.2018.1459956>.
45. Ko, K.; Cho, S.; Rao, R.R. Machine-Learning-Based Near-Surface Ozone Forecasting Model with Planetary Boundary Layer Information. *Sensors* **2022**, *22*, 7864. <https://doi.org/10.3390/s22207864>.
46. Oufdou, H.; Bellanger, L.; Bergam, A.; Khomsi, K. Forecasting Daily of Surface Ozone Concentration in the Grand Casablanca Region Using Parametric and Nonparametric Statistical Models. *Atmosphere* **2021**, *12*, 666. <https://doi.org/10.3390/atmos12060666>.
47. Jia, P.; Cao, N.; Yang, S. Real-Time Hourly Ozone Prediction System for Yangtze River Delta Area Using Attention Based on a Sequence to Sequence Model. *Atmos. Environ.* **2021**, *244*, 117917. <https://doi.org/10.1016/j.atmosenv.2020.117917>.
48. Juarez, E.K.; Petersen, M.R. A Comparison of Machine Learning Methods to Forecast Tropospheric Ozone Levels in Delhi. *Atmosphere* **2022**, *13*, 46. <https://doi.org/10.3390/atmos13010046>.

49. Colette, A.; Andersson, C.; Manders, A.; Mar, K.; Mircea, M.; Pay, M.T.; Raffort, V.; Tsyro, S.; Cuvelier, C.; Adani, M.; et al. EURODELTA-Trends, a Multi-Model Experiment of Air Quality Hindcast in Europe over 1990–2010. *Geosci. Model Dev.* **2017**, *10*, 3255–3276. <https://doi.org/10.5194/gmd-10-3255-2017>.
50. Derwent, R.G.; Davies, T.J. Modelling the Impact of NO<sub>x</sub> or Hydrocarbon Control on Photochemical Ozone in Europe. *Atmos. Environ.* **1994**, *28*, 2039–2052. [https://doi.org/10.1016/1352-2310\(94\)90472-3](https://doi.org/10.1016/1352-2310(94)90472-3).
51. Pavón-Domínguez, P.; Jiménez-Hornero, F.J.; Gutiérrez de Ravé, E. Proposal for Estimating Ground-Level Ozone Concentrations at Urban Areas Based on Multivariate Statistical Methods. *Atmos. Environ.* **2014**, *90*, 59–70. <https://doi.org/10.1016/j.atmosenv.2014.03.032>.
52. Hashim, N.M.; Noor, N.M.; Ul-Saufie, A.Z.; Sandu, A.V.; Vizureanu, P.; Deák, G.; Kheimi, M. Forecasting Daytime Ground-Level Ozone Concentration in Urbanized Areas of Malaysia Using Predictive Models. *Sustainability* **2022**, *14*, 7936. <https://doi.org/10.3390/su14137936>.
53. Silva, R.C.V.; Pires, J.C.M. Surface Ozone Pollution: Trends, Meteorological Influences, and Chemical Precursors in Portugal. *Sustainability* **2022**, *14*, 2383. <https://doi.org/10.3390/su14042383>.
54. Gardner, M.W.; Dorling, S.R. Artificial neural networks (the multilayer perceptron)—A review of applications in the atmospheric sciences; *Atmos. Environ.* **1998**, *32*, 2627–2636.
55. Lal, S.; Naja, M.; Subbaraya, B.H. Seasonal Variations in Surface Ozone and Its Precursors over an Urban Site in India. *Atmospheric Environ.* **2000**, *34*, 2713–2724.
56. Eliasson, I.; Thorsson, S.; Andersson-Sköld, Y. Summer Nocturnal Ozone Maxima in Göteborg, Sweden. *Atmos. Environ.* **2003**, *37*, 2615–2627. [https://doi.org/10.1016/S1352-2310\(03\)00205-X](https://doi.org/10.1016/S1352-2310(03)00205-X).
57. Murphy, J.G.; Day, D.A.; Cleary, P.A.; Wooldridge, P.J.; Millet, D.B.; Goldstein, A.H.; Cohen, R.C. The Weekend Effect within and Downwind of Sacramento-Part 1: Observations of Ozone, Nitrogen Oxides, and VOC Reactivity. *Atmos. Chem. Phys.* **2007**, *7*, 5327–5339.
58. Hakola, H.; Joffre, S.; Lättälä, H.; Taalas, P. Transport, Formation and Sink Processes behind Surface Ozone Variability in North European Conditions. *Atmos. Environ. Part A. Gen. Top.* **1991**, *25*, 1437–1447. [https://doi.org/10.1016/0960-1686\(91\)90003-P](https://doi.org/10.1016/0960-1686(91)90003-P).
59. Hsu, J.; Prather, M.J. Stratospheric Variability and Tropospheric Ozone. *J. Geophys. Res. Atmos.* **2009**, *114*, D06102. <https://doi.org/10.1029/2008JD010942>.
60. Balamurugan, V.; Balamurugan, V.; Chen, J. Importance of Ozone Precursors Information in Modelling Urban Surface Ozone Variability Using Machine Learning Algorithm. *Sci. Rep.* **2022**, *12*, 5646. <https://doi.org/10.1038/s41598-022-09619-6>.

**Disclaimer/Publisher’s Note:** The statements, opinions and data contained in all publications are solely those of the individual author(s) and contributor(s) and not of MDPI and/or the editor(s). MDPI and/or the editor(s) disclaim responsibility for any injury to people or property resulting from any ideas, methods, instructions or products referred to in the content.